



Original Article

Circular RNA Circ_0001322 inhibits gastric cancer progression by modulating the miR-1264/QKI axis and suppressing the Hedgehog pathway

Wenyi Wu^{1,2}, Yiqi Cai², Jinji Jin², Zhejing Chen², Mujian Teng^{1,*}¹ Department of Hepatobiliary Surgery 1st, Shandong Provincial Qianfoshan Hospital, Shandong University, Ji'nan, Shandong, 250013, China² Department of Gastrointestinal Surgery, The First Affiliated Hospital of Wenzhou Medical University, Wenzhou, Zhejiang, 325000, China

Article Info



Article history:

Received: January 18, 2024

Accepted: April 08, 2024

Published: May 31, 2024

Use your device to scan and read the article online



Abstract

Circular RNA hsa_circ_0001322 (circ1322) was demonstrated to be significantly reduced in expression in gastric cancer patients in our previous study, and changes in its expression were significantly correlated with lymph node metastasis. However, the underlying workings of circ1322 in gastric cancer are still not fully understood. Therefore, to confirm the effect of circ1322 on gastric cancer, we examined the expression of circ1322 in gastric cancer cells and tissues. The results showed that circ1322 was lowly expressed in GC tissues and cells. Subsequently, we further performed cellular assays and animal experiments, which showed that Circ1322 upregulation inhibited GC cell proliferation, migration and invasion, while promoting GC cell apoptosis, and inhibited tumor growth in mice. The direct targeting of circ1322 to miR-1264 was confirmed by bioinformatics prediction and validation of luciferase reporter gene assay. Circ1322 can act as a miR-1264 sponge to alleviate the inhibitory effect of miR-1264 on its target gene, QKI. miR-1264 regulates the expression of QKI and the activity of the hedgehog pathway. That is, circ1322 may act as a competing endogenous RNA (ceRNA) to inhibit the hedgehog pathway by targeting the miR-1264/QKI axis, which in turn promotes GC progression.

Keywords: hsa_circ_0001322, miR-1264, QKI, Hedgehog pathway, Gastric cancer

1. Introduction

Gastric cancer (GC) is a significant focus of clinical and basic research, that is characterized by high aggressiveness, heterogeneity, and poor prognosis. According to estimates from the United States Cancer Statistics registry, worldwide, there were 1.08 million new cases of GC and 0.77 million deaths related to GC [1]. Although considerable progress has been made in the treatment of GC, the presence of high intratumor and intratumoral heterogeneity, late diagnosis, and the development of chemotherapy resistance continue to hinder improvements in GC-related survival [2, 3].

Circular RNA (circRNA) is a class of single-stranded transcripts generated by the back-splicing process [4]. Due to its covalently closed loop structure, circRNA exhibits high stability and is significantly abundant in plasma, making it an efficient biomarker itself [5]. In recent years, there have been significant developments in transcriptomics, leading to the discovery of an increasing number of functional circRNAs. These circRNAs perform various biological functions, such as acting as transcriptional and

splicing regulators [6], protein templates [7], and protein scaffolds [8]. What's more, the role of circRNA as a "microRNA (miRNA) sponge" is widely reported in tumors. For example, in GC cells, circNRIP1 functions as a competitive endogenous RNA for miRNA-149-5p to regulate the classical signaling pathway AKT/mTOR axis [9]. CircCUL2 competes with miR-142-3p for binding sites, thereby regulating autophagy activation and impacting cisplatin resistance in GC [10]. Circ_0005758 can target the miR-1229-3p/GCNT4 feedback loop, thereby impeding the progression of GC [11]. Hsa_circ_0001322 is a novel circRNA, formed by reverse splicing of exon 3 to 8 of the eukaryotic initiation factor 4E3 (eIF4E3) gene. Interestingly, in our previous studies, circ_0001322 has been found to have potential as a marker for the diagnosis and metastasis of GC [12]. Low expression of circ_0001322 was observed in GC tissues and exhibited a negative correlation with lymph node metastasis (ROC: sensitivity: 90%, specificity: 75%). However, the function of circ_0001322 in GC has not yet been studied.

The Hedgehog (Hh) signaling pathway, as a classical

* Corresponding author.

E-mail address: tengmujian2007@163.com (M. Teng).Doi: <http://dx.doi.org/10.14715/cmb/2024.70.5.27>

developmental signaling pathway, plays a crucial role in gastrointestinal organogenesis, and mutations in its core ligand members can result in a spectrum of intestinal abnormalities, such as gut malrotation, annular pancreas, duodenal stenosis, and Hirschsprung's disease [13-15]. When the Hh signal is abnormally activated, it may play a role in the formation and growth of tumors through autocrine and paracrine effects. It is worth mentioning that chronic infection with *H. pylori* has become a significant initial event in the occurrence of GC [16, 17]. Infection-induced spasmolytic polypeptide-expressing metaplasia (SPeM), a type of atrophy in the acid gland, requires standardized Hh signaling [18]. In the case of bacterial infection, Hh signaling may be necessary to polarize a particular subset of myeloid cells and transition the gastric mucosa from a pro-inflammatory state to a pre-tumor state [19]. Targeting the Hh signaling pathway remains the primary focus for the treatment of human GC. Sulforaphane exerts its anticancer effects by suppressing the Hh signaling pathway to GC stem cells [20]. miRNA-150/Sufu promotes cell proliferation, migration, and epithelial-mesenchymal transformation through dual activation of Hh and Wnt signaling [21]. Otherwise, preclinical data on certain small molecule inhibitors have provided evidence of the crosstalk between Hh signaling and cytokines during the precancerous stage, but, clinical trial results have been less than satisfactory. Therefore, accurate biomarkers are needed to identify subpopulations that can benefit from Hh inhibition.

In this study, we hypothesized that circ_0001322 was involved in regulating the progression of GC and, therefore, aimed to investigate its exact function in GC.

2. Materials and Methods

2.1. Tissue samples

The study was approved by the Ethics Committee of the First Affiliated Hospital of Wenzhou Medical University. A total of 29 patients with GC who were diagnosed for the first time in our hospital and did not receive radiotherapy/chemotherapy before surgery were enrolled. All patients, who were notified before, signed written informed consent. GC tissue and paracancerous tissue (normal) specimens were collected under HIPAA protocol and stored in liquid nitrogen.

2.2. Cell lines

The human GC cell lines, including HGC-27 (TCHu22), MKN-45, NCI-N87 (TCHu130), AGS (TCHu232), and SUN-1 (TCHu230), were obtained from the Cell Bank of the Chinese Academy of Sciences. The GES-1 human normal gastric mucosal epithelial cell line served as the control group. All cells were cultured in RPMI 1640 medium (11875093, GIBCO), containing 10% fetal bovine serum (FBS, C04001-500, Viva Cell, Shanghai, China) and 1% penicillin-streptomycin (15140148, Gibco, USA), and maintained at 37°C with 5% CO₂.

2.3. RT-qPCR

Total RNA, extracted from tissues and cells by TRIzol reagent was used as a template to synthesize cDNA. The amplification reaction was performed on a Roche Light-Cycler® 480II RT-qPCR instrument (Roche Molecular Biochemicals, Mannheim, Germany) using the TB Green Premix EX Taq. Relative expression of circ-0001322 and miR-1264 were quantified by the 2^{-ΔΔCt} method.

2.4. Bioinformatics prediction

Circbank and Circinteratome websites were utilized to predict the potential downstream miRNAs of circ_0001322. Similarly, miWalk, microT-CDS, TargetScan, and Survival websites were employed to identify the targets of miRNAs.

2.5. Lentivirus RNAi construction and infection

According to the basic information of circ-0001322, overexpression and interference sequences (CCACAGTT-TGGAAAGAGTTGCTGTT) were designed, and were synthesized from Shanghai GenePharma (China), where the overexpression sequence was constructed into the lentiviral vector JS043 at the XhoI cloning site using enzymatic ligation (15224041, Corning, NY, USA), yielding the overexpression recombinant plasmid (pc-circ1322); similarly, the interference sequence was constructed into the lentiviral vector JS039 at the EcoRI and BamHI cloning sites using the same method, resulting in the interference recombinant plasmid (sh-circ1322). The negative controls set were pc-DNA and sh-NC, respectively. Plasmid amplification was performed using an *E. coli* cell receptive state, followed by an extraction kit.

The log-growing 293T cells were seeded into 6-well plates and cultured in DMEM medium (C3113-0500, Viva Cell) supplement with 10% FBS, F-12 (HAM) Nutrient Mixture (01-095-1A, Viva Cell) and 1% penicillin-streptomycin for 20 hours. Target plasmids pc-circ_0001322, pc-DNA, sh-circ0001322, and sh-NC were individually transfected into 293T cells using Lipofectamine 3000, followed by a 6-hour incubation in serum-free medium and subsequent replacement with complete medium for an additional 48-hour culture. The collected lentiviruses were then obtained through ultracentrifugation.

MKN-45 and AGS cells were seeded separately into petri dishes, and the corresponding viruses were added to infect the cells. After 72 hours, the cells were screened using puromycin (Sigma, Germany) to observe the infection efficiency by RT-qPCR.

2.6. Cell transfection

GP-transfect-Mate (G04008, GenePharma, Shanghai, China) and miR-1264 mimics (CAAGUCUUAUUUGA-GCACCUGUU) or miR-1264 inhibitor (CAGGUGCU-CAAUAAGACUUGUG) were mixed and incubated in serum-free conditions for 20 minutes to form transfection complexes; subsequently, the complexes were added to pre-seeded cells in a 6-well plate and incubated for 4 hours followed by replacement with complete medium for a further 48-hour culture.

The PCR product of QKI was cloned into the linear plasmid JS036 at the EcoRI and HindIII restriction sites, resulting in the recombinant plasmid JS036-QKI; similarly, QKI overexpression plasmid was transfected into cells using GP-Transfect-Mate transfection reagent.

2.7. Dual-luciferase reporter assay

To verify the combination between circ_0001322 (or QKI) and miR-1264, the wild-type or mutant sequences (QKI 3'UTR) containing the binding sites were constructed into psiCHECK-2 plasmid at the XhoI cloning site. Subsequently, reporter plasmids plus miR-1264 mimics were co-transfected in cells using Lipofectamine 3000 reagent for 24 hours. Plasmids plus miR-NC was used as

a negative control. The calculation of relative luciferase activity involved comparing the activities of both Renilla and firefly luciferase (Promega).

2.8. CCK-8 assay

After being transfected, the GC cells were re-suspended and subsequently seeded into 96-well plates, with each well containing 2,000 cells. A CCK-8 kit was used to assess the proliferative capacity of cells. A 10 μ L dose of CCK-8 reagents was added to the cells at the specified time points (0, 24, 48, 72, and 96 hours), and continually incubated for 2 hours. The optical density (OD) value was determined by utilizing the Bio Tek Synergy instrument (Winooski, Vermont, USA) at a wavelength of 450 nm.

2.9. Cell migration and invasion assays

Transwell was performed to assess the impacts of circ_0001322 expressions on migration and invasion. A total of 50,000 stable transfected cells were introduced into the upper chambers, which were filled with serum-free medium, and the lower chambers were filled with medium containing 10% FBS, which served as a chemoattractant. Different from migration assays, the upper chambers for invasion assays need to be coated with Matrigel in advance at 4 °C overnight. After incubation for 24 to 48 hours, the cells were fixed with 4% paraformaldehyde (PFA) and subsequently stained with 0.1% crystal violet (C02121, Beyotime). Afterward, the fields were photographed, and the number of cells was counted using a microscope.

2.10. Animal-Xenograft tumor models

Nude mice are the classic materials for xenograft tumor experiments. We purchased 48 male nude mice (4 weeks old) with a BALB/c background from the Animal Experimental Center of Hubei Province (Wuhan, China) for the experiment. After 1 week of adaptive culture, the mice were randomly divided into two groups: the MKN-45 group (consisting of pc-DNA, pc-circ_0001322, sh-NC, si-circ_0001322, with 6 mice per group) and the AGS group (also consisting of pc-DNA, pc-circ_0001322, sh-NC, si-circ_0001322, with 6 mice per group). Briefly, each group of mice was, respectively, injected into the underarms with MKN-45/AGS cell suspension (5,000,000). Tumor volume, which was monitored every five days using a caliper, was calculated using the following formula: tumor volume = (length \times width²)/2. After thirty days, the mice were euthanized with 120 mg/kg Nembutal, and the xenograft tumors were collected for subsequent weighing.

2.11. Colony formation assay

Stable transfected MKN-45 and AGS cells were re-suspended, and then uniformly seeded onto 6-well plates at a density of 3,000 cells/well, respectively. The cells were continuously cultured for one week until the cell number reached greater than 50 in a single clone, with medium change and observation of cell status every three days. After cloning, all aforementioned cells were fixed and stained in preparation for subsequent photography and counting.

2.12. Apoptosis

The transfected MKN-45 and AGS cells (300,000) were resuspended with 5 μ L of Annexin V-FITC and 10 μ L of PI (40310ES50, YEASEN, Shanghai, China) and incu-

bated for 15 minutes, followed by analysis using FACS-Canto II flow cytometry (BD, USA).

2.13. Radioimmunoprecipitation (RIP)

The RIP assay was carried out to verify the direct combination of circ-0001322 and miR-1264, miR-1264, and QKI. The transfected MKN-45 and AGS cells (300,000) were resuspended in RIP lysate (LOT3159044, Merck, Germany) containing RNase inhibitor and PI and left to break for 8 minutes. After being centrifuged, the supernatant was separated into three categories: input, IgG, and Ago2 groups. Individual Ago2 (2897S, CST, Danvers, MA, USA) and IgG (3900S, CST) antibodies were added to the corresponding group. Following the attachment of the antibodies to the beads, the antigen was introduced. Eventually, the RNA was gathered for subsequent RT-qPCR.

2.14. Western blot

Western blot was conducted to evaluate the level of the Hh pathway signaling pathway. The specific protein antibodies information used were anti-QKI (DF12715, Affinity, USA), anti-PTCH1 (CY1243, Abways, Shanghai, China), anti-SMO (66851-1-Ig, Proteintech, USA), anti-GLI1 (DF7523, Affinity) and anti-GAPDH (AB0037, Abways). As previously described, the transfected cells were cleaved in a RIRA lysate (P0013, Beyotime) containing PMSF (G2008-1ML, Servicebio, Wuhan, China) and PI, followed by concentration determination (P0010, Beyotime). The protein samples denatured at 95°C were electrophoretically separated on a pre-configured SDS-PAGE gel, and subsequently electrically transferred to a PVDF membrane. To block the membranes, a solution of 5% skim milk was employed and left at room temperature for an hour. The primary antibody was incubated at 4°C overnight, and the corresponding second antibody was replaced the next day, and incubated at room temperature for 1 hour. Finally, an enhanced chemiluminescence system (G2014-50ML, Servicebio) was used to detect protein expression.

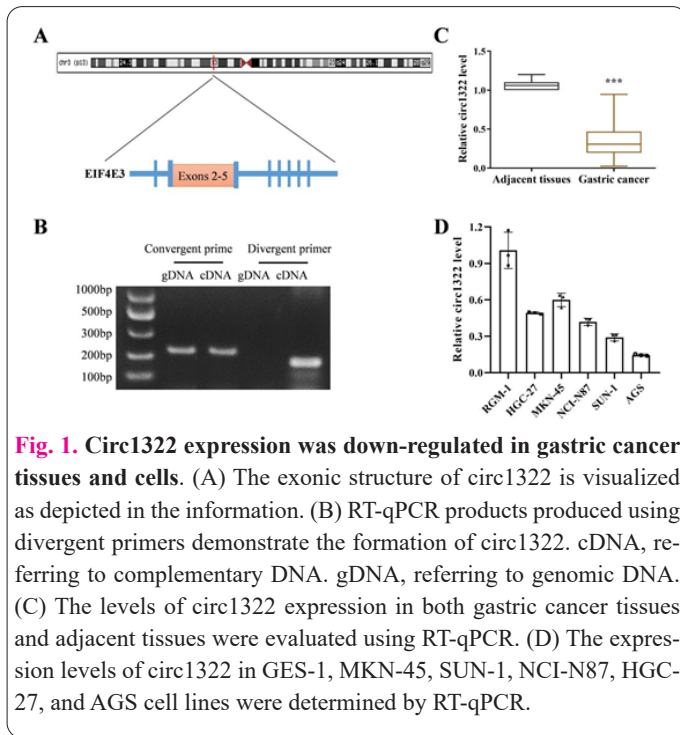
2.15. Statistical methods

The experiments were conducted independently, with a minimum of three repetitions. The data were presented as mean \pm standard deviation and analyzed using SPSS 19.0 software. The comparison between the two groups was carried out using a two-tailed paired Student's *t*-test, and the comparison of differences among multiple groups was conducted using a one-way ANOVA, followed by Tukey's post hoc test applied afterward. Pearson's correlation analysis based on cancer tissue was applied for the correlation analysis between hsa_circ_0001322 and miR-1264. Any value of *P* < 0.05 was considered statistically significant.

3. Results

3.1. Circ_0001322 expressions are decreased in gastric cancer tissues and cell lines

The database shows that circ1322 is formed by the circularization of exons 2-5 of the EIF4E3 gene, the spliced length of which is 609bp (Fig. 1A). To demonstrate the circular nature of circ1322 instead of it being linear, we developed divergent and convergent primers for circ1322 and its corresponding linear mRNA. Subsequently, both cDNA and gDNA were subjected to nucleic acid electrophoresis, which revealed that circ1322 displays a circu-



lar form rather than a linear one, as depicted in Fig. 1B. The RT-qPCR results revealed a noteworthy decline in the expression of circ1322 in GC tumor tissues as opposed to adjacent tissues (Fig. 1C). We then proceeded to confirm the reduced levels of circ1322 in kinds of GC cell lines, namely HGC-27, MKN-45, NCI-N87, AGS, and SUN-1, in comparison to GES-1 cells. Out of all the cell lines, MKN-45 cells demonstrated the highest level of circ1322 expression, whereas AGS cells displayed the least amount (Fig. 1D). Consequently, we opted to focus on MKN-45 and AGS GC cells for exploring the function of circ1322.

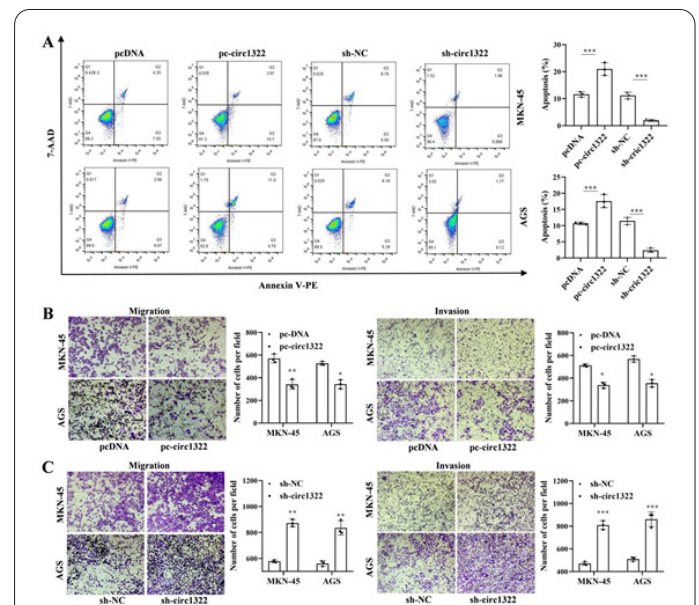
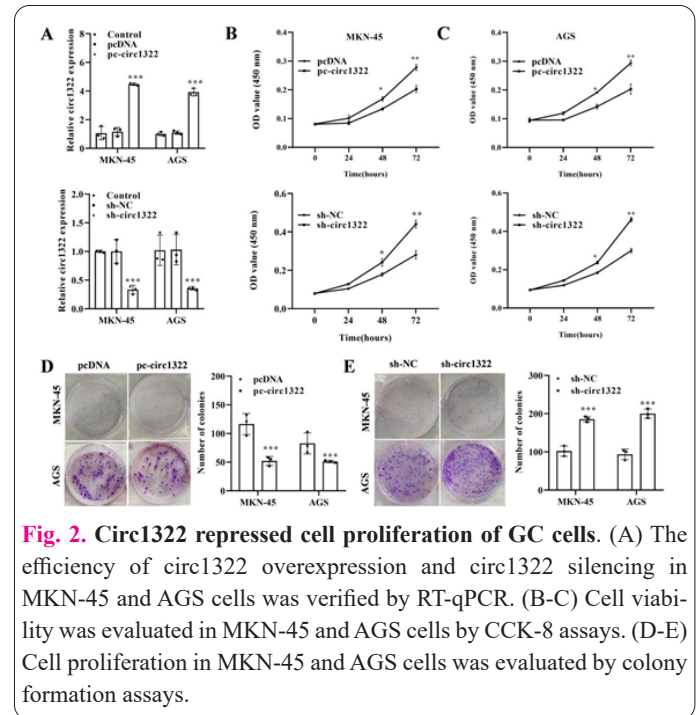
3.2. Circ1322 hinders the progression of gastric cancer

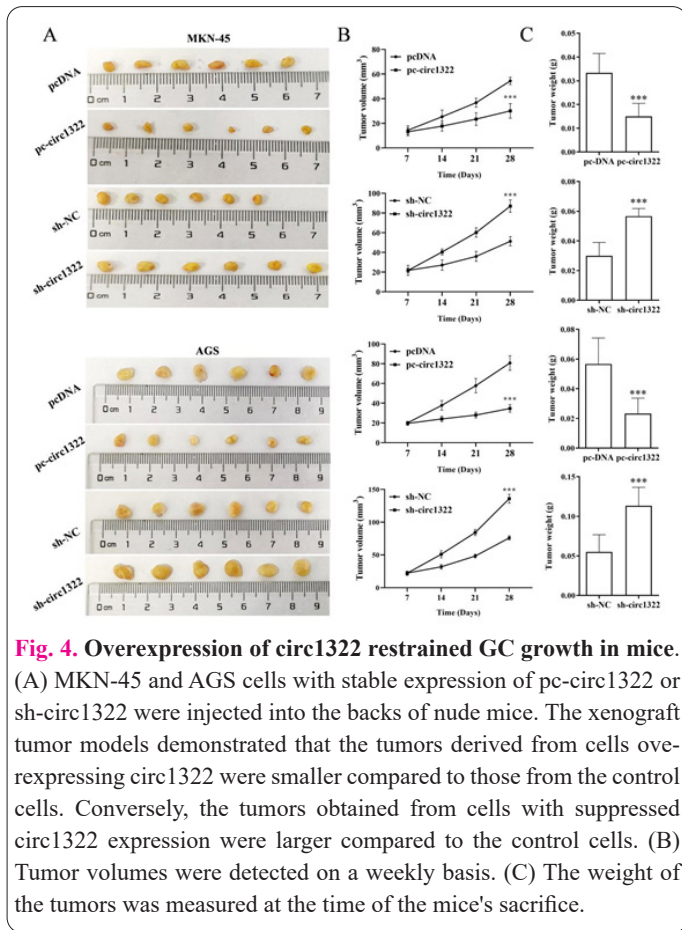
To study the function of circ1322 in GC, the expression of circ1322 was overexpressed and downregulated respectively in the MKN-45 and AGS cell lines, through transfected with circ1322 overexpression plasmids or lentiviral plasmids. The efficiency of circ1322 overexpression and silencing was confirmed in MKN-45 and AGS cells through RT-qPCR analysis (Fig. 2A). Cell viability was assessed in MKN-45 and AGS cells using CCK-8 assays. The overexpression of circ1322 led to a reduction in cell viability in both MKN-45 and AGS cells. In contrast, an increase in cell viability was observed when the expression of circ1322 was reduced (Fig. 2B-C). The results from subsequent colony formation assays further validated that the overexpression of circ1322 suppressed cell proliferation in both MKN-45 and AGS cells, while the downregulation of circ1322 enhanced cell proliferation (Fig. 2D). Additionally, the apoptosis assays indicated that the upregulation of circ1322 facilitated apoptosis, whereas the downregulation of circ1322 inhibited apoptosis in GC cells (Fig. 3A). The metastatic and invasive capacities of GC cells were assessed through transwell assays. The increased expression of circ1322 hindered the metastatic and invasive potential of both MKN-45 and AGS cells, whereas the decreased expression of circ1322 enhanced their metastatic and invasive capabilities (Fig. 3B-C). To further confirm the *in vivo* role of circ1322, MKN-45 or AGS cells that stably expressed pc-circ1322 or sh-

circ1322 were introduced into the backs of nude mice. The xenograft tumor models have shown that the tumors derived from cells having overexpression of circ1322 were of reduced size and had a lower weight in comparison to the tumors obtained from the control cells. Conversely, the tumors obtained from cells with circ1322 knockdown were characterized by larger size and heavier weight in comparison to the control cells (Fig. 4). The above results proved that circ1322 restrained gastric tumor growth.

3.3. Circ1322 serves as a miRNA sponge of hsa-miR-1264

Numerous researchers have confirmed that circRNA functions as a “miRNA sponge”, controlling tumor deve-





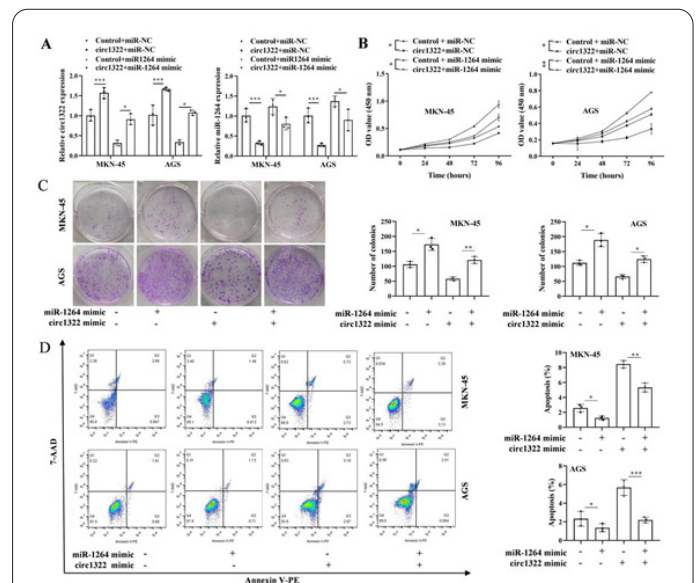
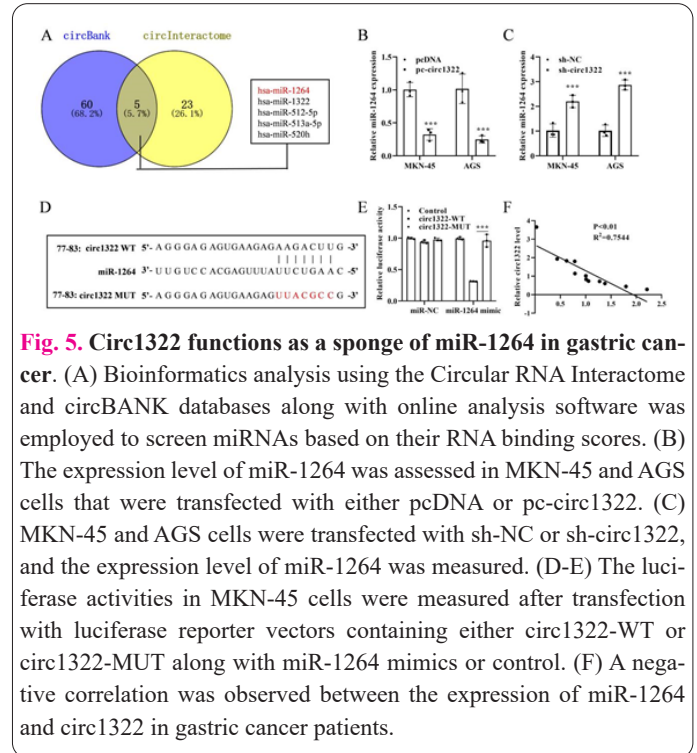
lopment regulation. Moreover, circRNA can control gene expression downstream as well. To identify the target miRNAs of circ1322, a comprehensive analysis was conducted across the prediction databases of circBANK and Circular RNA Interactome to screen miRNAs by considering their RNA binding scores. It was revealed that circ1322 had the potential to act as a sponge for hsa-miR-1264, hsa-miR-1322, hsa-miR-512-5p, hsa-miR-513a-5p, and hsa-miR-520h (Fig. 5A). Afterward, in MKN-45 and AGS cells expressing pc-circ1322 or sh-circ1322, only hsa-miR-1264 exhibited a significant change in expression levels (Fig. 5B-C). It was suggested that circ1322 might potentially serve as a sponge for miR-1264. To confirm the absorption of miR-1264 and circ1322, a dual-luciferase reporter assay was carried out to ascertain the direct binding between circ1322 and miR-1264, relying on their complementary sequences (Fig. 5D). Plasmids containing the wild-type sequence (circ1322-WT) and the mutant binding site sequence (circ1322-MUT) were created. These plasmids were subsequently co-transfected, along with either the miR-1264 mimic or miR-NC, into MKN-45 cells.

The results suggest a significant decrease in luciferase activity of the circ1322-WT when miR-1264 mimics were introduced. However, the luciferase activity of the empty vector or the circ1322-MUT vector remained unaffected (Fig. 5E), validating the direct interaction of miR-1264 with circ1322. Furthermore, we analyzed to examine the relationship between circ1322 and miR-1264 in GC tissues, where we observed a negative correlation between their expressions (Fig. 5F).

To ascertain the effect of circ1322 on gastric cancer by interacting with miR-1264, gain-of-function experiments were performed. The formation of four groups, namely control + miR-NC, circ1322 + miR-NC, control + miR-

1264 mimic, and circ1322 + miR-1264, was achieved by transfecting MKN-45 and AGS cells with either circ1322 or miR-1264 mimic. After transfection, the expression of circ1322 and miR-1264 was verified using RT-qPCR (Fig. 6A).

The cells that were transfected were placed in an incubator for 96 hours, after which their viability was assessed using CCK-8 assays. The results indicated that the cell viability of MKN-45 and AGS cells was decreased when circ1322 was overexpressed and enhanced when miR-



1264 mimic, and circ1322 + miR-1264, was achieved by transfecting MKN-45 and AGS cells with either circ1322 or miR-1264 mimic. After transfection, the expression of circ1322 and miR-1264 was verified using RT-qPCR (Fig. 6A).

The cells that were transfected were placed in an incubator for 96 hours, after which their viability was assessed using CCK-8 assays. The results indicated that the cell viability of MKN-45 and AGS cells was decreased when circ1322 was overexpressed and enhanced when miR-

1264 was overexpressed, as opposed to the control group. On the other hand, when cells were overexpressing miR-1264, the up-regulation of circ1322 was able to counteract the detrimental effect on cell viability caused by miR-1264 (Fig. 6B). The results were further strengthened by subsequent colony formation assays and apoptosis assays, verifying the contradictory roles of miR-1264 and circ1322, as illustrated in Fig. 6C-D, respectively.

3.4. The circ1322-miR-1264/QKI axis is accountable for the modified metabolism in GC cells through the hedgehog pathway

The miR-1264-associated genes, LART and QKI, were pinpointed by employing miWalk, microT-CDS, TargetScan, and the GPAA2 database (Fig. 7A). To ascertain the binding potential of their mRNA with miR-1264, an RIP assay was performed in MKN-45 cells for evaluation purposes. There was a considerable increase in the mRNA level of QKI in the Ago2 antibody group when compared to the IgG control group (Fig. 7B). The MKN-45 and AGS cells were transfected with either the miR-1264 mimic or the miR-1264 inhibitor. Changes in the levels of QKI protein expression were assessed using Western blotting. It was discovered that the excessive expression of miR-1264 led to a decrease in QKI protein expression, whereas the reduction of miR-1264 increased QKI protein expression (Fig. 7C). Then, plasmids were created that contained the normal sequence (QKI-WT) or the altered binding site sequence (QKI-MUT) (Fig. 7D). The plasmids were later combined with either the miR-1264 mimic or miR-NC and transfected together into MKN-45 cells, facilitating the conduct of a dual luciferase reporter assay. The results indicate that the high expression of miR-1264 significantly reduced the luciferase activity of the vector containing

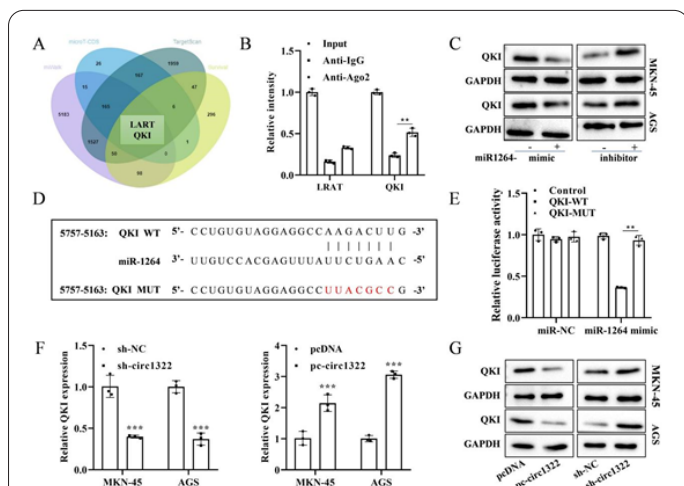


Fig. 7. QKI was identified as the direct gene affected by miR-1264.

(A) Through the use of miWalk, microT-CDS, TargetScan, and the GPAA2 database, two potential genes associated with miR-1264 were discovered. (B) MKN-45 cells were subjected to RIP experiments to evaluate the binding of miRNA to mRNA, followed by RT-qPCR analysis. (C) The mRNA and protein expression levels of QKI in MKN-45 and AGS cells that were transfected with miR-1264 mimics were assessed. (D-E) After transfection with luciferase reporter vectors containing QKI-WT or QKI-MUT and either miR-1264 mimics or control, the relative activities of luciferase were measured in MKN-45 cells. (F-G). The expression of QKI mRNA and protein in MKN-45 and AGS cells was detected after transfection with either pc-circ1322 or sh-circ1322 vectors

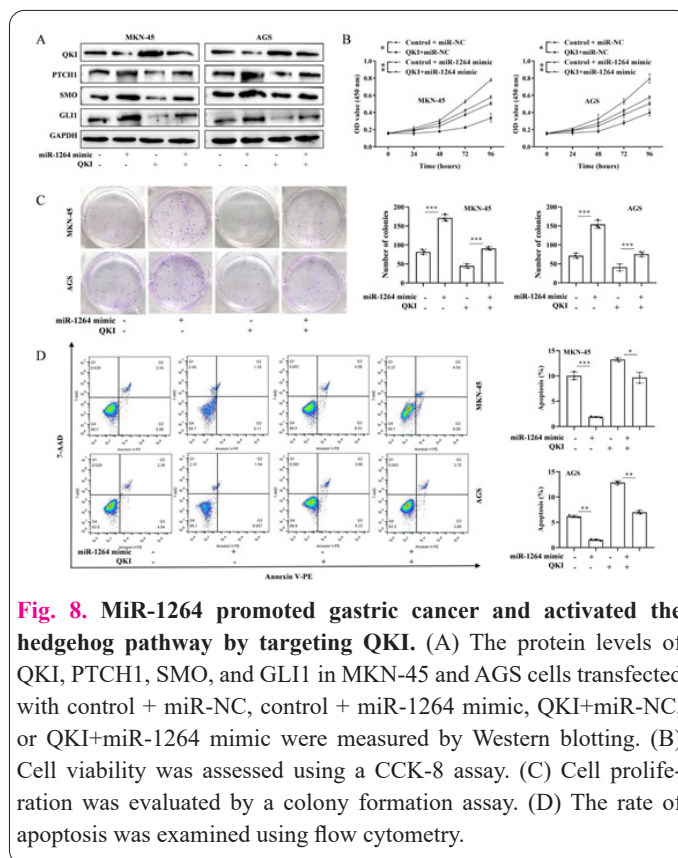


Fig. 8. MiR-1264 promoted gastric cancer and activated the hedgehog pathway by targeting QKI. (A) The protein levels of QKI, PTCH1, SMO, and GLI1 in MKN-45 and AGS cells transfected with control + miR-NC, control + miR-1264 mimic, QKI+miR-NC, or QKI+miR-1264 mimic were measured by Western blotting. (B) Cell viability was assessed using a CCK-8 assay. (C) Cell proliferation was evaluated by a colony formation assay. (D) The rate of apoptosis was examined using flow cytometry.

QKI-WT. Nevertheless, no decline was detected in the luciferase activity of either the empty vector or the vector incorporating QKI-MUT (Fig. 7E). This solidifies the connection between miR-1264 and QKI, confirming that miR-1264 directly regulates the functioning of QKI. The mRNA and protein expression levels of QKI were examined in MKN-45 and AGS cells that were transfected with either pc-circ1322 or sh-circ1322 vectors. Overexpression of circ1322 resulted in increased QKI expression levels in both MKN-45 and AGS cells, whereas downregulation of circ1322 led to a decrease in QKI expression levels (Fig. 7F-G).

Next, we proceeded to examine the protein expression levels of QKI, PTCH1, SMO, and GLI1 in MKN-45 and AGS cells that were transfected with different treatments: control + miR-NC, control + miR-1264 mimic, QKI + miR-NC, or QKI + miR-1264 mimic. The results showed that transfection of miR-1264 mimic increased the expression levels of PTCH1, SMO, and GLI1, which were reduced by overexpression of circ1322 (Fig. 8A). Cell viabilities of MKN-45 and AGS cells transfected with miR-1264 mimic were elevated, which were inhibited when QKI was overexpressed (Fig. 8B). Colony formation and apoptosis assays further conformed to the role of the hedgehog pathway and QKI in the GC cells (Fig. 8C-D). These results indicated that MiR-1264 promoted gastric cancer and activated the hedgehog pathway by targeting QKI.

4. Discussion

In our previous study, we discovered that circ1322 exhibited relatively low expression levels in gastric cancer tissues. Moreover, we observed a significant correlation between changes in circ1322 expression and lymph node metastasis [12]. In this current study, we aimed to delve deeper into the specific mechanism of circ1322 in gastric cancer. Initially, we utilized bioinformatics predic-

tion and RNA immunoprecipitation techniques to ascertain whether miR-1264 functions as a binding miRNA for circ1322. Subsequently, we confirmed their complementary binding through the dual luciferase assay. It has been reported that miR-1264 regulates the expression of QKI, which affects the progression of triple-negative breast cancer [22]. QKI, an RNA-binding protein, has been extensively linked with the development of various types of cancer [23, 24]. In addition, some studies have observed a substantial decrease in the expression of QKI within gastric cancer tissues, and the expression of QKI has been identified as an independent prognostic factor that impacts patient survival [25]. The impairment of QKI activates the hedgehog signaling pathway, resulting in a unique mechanism through which glioblastoma stem cells maintain their stemness [26]. Thus, we aimed to comprehend the intricate tumor promotion mechanism that lies beneath the circ1322/miR-1264/QKI axis via the hedgehog pathway.

Based on our experiments and analysis, we have observed that the overexpression of circ1322 effectively blocked the proliferation, migration, invasion, and miR-1264 expression in gastric cancer cells, while also promoting apoptosis. Additionally, circ1322 overexpression successfully suppressed tumor growth in the PDX model. On the other hand, miR-1264 restrained the expression of circ1322 in gastric cancer cells, and its overexpression hindered the favorable behavior of circ1322. Moreover, we have shown that QKI overexpression counteracted the impacts of miR-1264 and inhibited the hedgehog pathway.

CircRNAs are produced by reverse splicing, which links specific sites together to form a closed loop. They serve as regulators of gene expression at multiple levels and are implicated in various disease processes including alternative splicing, miRNA regulation, transcription regulation, protein sequestration, and even protein-coding [27]. This indicates that circRNAs can function as both tumor suppressor genes and oncogenes in the context of tumor development. Several studies have shown that certain circRNAs can regulate the expression of tumor suppressor or initiator genes through their miRNA sponge function, thereby affecting biological processes [28-30]. Furthermore, circRNAs can modulate gene expression by forming RNA-protein complexes through their interaction with RNA-binding proteins [31]. In our study, we showed that circ1322 acts as a sponge absorbing miR-1264 to modulate QKI expression in GC.

CircRNAs possess exceptional stability and display resistance to degradation, making them ideal biomarkers for diagnostic use. They can be easily detected in bodily fluids such as plasma and gastric juice, offering a minimally invasive method for diagnosing gastric cancer. Analysis of circRNA expression in patients with gastric cancer has revealed distinct circRNAs like circSFMBT2, circHIPK3, and circNRIP1, which exhibit substantial upregulation in gastric cancer [27]. Consequently, these circRNAs hold promise as potential biomarkers for identifying the disease. By understanding the function of circRNAs as miRNA sponges, we can better understand the regulatory mechanisms during tumor development and discover new therapeutic targets and treatment strategies. However, the current understanding of this mechanism is still relatively limited, and further studies are needed to reveal its mechanism of action and reliability, as well as the potential application prospects in tumor therapy.

5. Conclusion

In summary, our study presents evidence indicating that hsa_circ_0001322 exhibits low expression levels in gastric cancer tissues. In addition, it serves as a regulator in the processes of cell proliferation, migration, invasion, and apoptosis. In terms of its mechanism, hsa_circ_0001322 acts as a competitive ceRNA for miR-1264, controlling the expression of QKI and simultaneously triggering the activation of the hedgehog signaling pathway. Consequently, Hsa_circ_0001322 holds the potential to serve as a biomarker for predicting GC prognosis.

Funding

The authors declare that no funds, grants, or other support were received during the preparation of this manuscript.

Competing Interests

The authors have no relevant financial or non-financial interests to disclose.

Author Contributions

MT contributed to the study conception and design. Material preparation, data collection and analysis were performed by WW, YC, JJ and ZC. The first draft of the manuscript was written by WW and all authors commented on previous versions of the manuscript. All authors read and approved the final manuscript.

Data Availability

All data generated or analyzed during this study are included in this manuscript.

Ethics approval

This study was approved by the Ethics Committee of the First Affiliated Hospital of Wenzhou Medical University.

Consent to participate

Written informed consent was obtained from each patient.

Consent to publish

Not applicable.

References

1. Sung H, Ferlay J, Siegel RL, Laversanne M, Soerjomataram I, Jemal A, Bray F (2021) Global Cancer Statistics 2020: GLOBOCAN Estimates of Incidence and Mortality Worldwide for 36 Cancers in 185 Countries. *CA Cancer J Clin* 71 (3): 209-249. doi: 10.3322/caac.21660
2. Sexton RE, Al Hallak MN, Diab M, Azmi AS (2020) Gastric cancer: a comprehensive review of current and future treatment strategies. *Cancer Metastasis Rev* 39 (4): 1179-1203. doi: 10.1007/s10555-020-09925-3
3. Onoyama T, Ishikawa S, Isomoto H (2022) Gastric cancer and genomics: review of literature. *J Gastroenterol* 57 (8): 505-516. doi: 10.1007/s00535-022-01879-3
4. Kristensen LS, Andersen MS, Stagsted LVW, Ebbesen KK, Hansen TB, Kjems J (2019) The biogenesis, biology and characterization of circular RNAs. *Nat Rev Genet* 20 (11): 675-691. doi: 10.1038/s41576-019-0158-7
5. Vo JN, Cieslik M, Zhang Y, Shukla S, Xiao L, Zhang Y, Wu YM, Dhanasekaran SM, Engelke CG, Cao X, Robinson DR, Nesvizhskii AI, Chinnaiyan AM (2019) The Landscape of Circular RNA in Cancer. *Cell* 176 (4): 869-881 e813. doi: 10.1016/j.

- cell.2018.12.021
6. Li Z, Huang C, Bao C, Chen L, Lin M, Wang X, Zhong G, Yu B, Hu W, Dai L, Zhu P, Chang Z, Wu Q, Zhao Y, Jia Y, Xu P, Liu H, Shan G (2015) Exon-intron circular RNAs regulate transcription in the nucleus. *Nat Struct Mol Biol* 22 (3): 256-264. doi: 10.1038/nsmb.2959
 7. Pamudurti NR, Bartok O, Jens M, Ashwal-Fluss R, Stottmeister C, Ruhe L, Hanan M, Wylter E, Perez-Hernandez D, Ramberger E, Shenzen S, Samson M, Dittmar G, Landthaler M, Chekulaeva M, Rajewsky N, Kadener S (2017) Translation of CircRNAs. *Mol Cell* 66 (1): 9-21 e27. doi: 10.1016/j.molcel.2017.02.021
 8. Zhou WY, Cai ZR, Liu J, Wang DS, Ju HQ, Xu RH (2020) Circular RNA: metabolism, functions and interactions with proteins. *Mol Cancer* 19 (1): 172. doi: 10.1186/s12943-020-01286-3
 9. Zhang X, Wang S, Wang H, Cao J, Huang X, Chen Z, Xu P, Sun G, Xu J, Lv J, Xu Z (2019) Circular RNA circNRIP1 acts as a miRNA-149-5p sponge to promote gastric cancer progression via the AKT1/mTOR pathway. *Mol Cancer* 18 (1): 20. doi: 10.1186/s12943-018-0935-5
 10. Peng L, Sang H, Wei S, Li Y, Jin D, Zhu X, Li X, Dang Y, Zhang G (2020) circCUL2 regulates gastric cancer malignant transformation and cisplatin resistance by modulating autophagy activation via miR-142-3p/ROCK2. *Mol Cancer* 19 (1): 156. doi: 10.1186/s12943-020-01270-x
 11. Li P, Xiao W (2022) Circ_0005758 impedes gastric cancer progression through miR-1229-3p/GCNT4 feedback loop. *Toxicol In Vitro* 85: 105454. doi: 10.1016/j.tiv.2022.105454
 12. Wenyi W, Yongyu B, Xiaopeng Z, Yiqi C, Zhuha Z, Xiaojiao R (2022) Expression of hsa_circ_0001322 in gastric cancer and its clinical significance. *Journal of Wenzhou Medical University* 52 (2): 104-108. doi:
 13. Ramalho-Santos M, Melton DA, McMahon AP (2000) Hedgehog signals regulate multiple aspects of gastrointestinal development. *Development* 127 (12): 2763-2772. doi: 10.1242/dev.127.12.2763
 14. Kim SK, Melton DA (1998) Pancreas development is promoted by cyclopamine, a hedgehog signaling inhibitor. *Proc Natl Acad Sci U S A* 95 (22): 13036-13041. doi: 10.1073/pnas.95.22.13036
 15. Litingtung Y, Lei L, Westphal H, Chiang C (1998) Sonic hedgehog is essential to foregut development. *Nat Genet* 20 (1): 58-61. doi: 10.1038/1717
 16. Salvatori S, Marafini I, Laudisi F, Monteleone G, Stolfi C (2023) Helicobacter pylori and Gastric Cancer: Pathogenetic Mechanisms. *Int J Mol Sci* 24 (3). doi: 10.3390/ijms24032895
 17. Cheng HC, Yang YJ, Yang HB, Tsai YC, Chang WL, Wu CT, Kuo HY, Yu YT, Yang EH, Cheng WC, Chen WY, Sheu BS (2023) Evolution of the Correa's cascade steps: A long-term endoscopic surveillance among non-ulcer dyspepsia and gastric ulcer after H. pylori eradication. *J Formos Med Assoc* 122 (5): 400-410. doi: 10.1016/j.jfma.2022.11.008
 18. Goldenring JR, Nam KT (2010) Oxyntic atrophy, metaplasia, and gastric cancer. *Prog Mol Biol Transl Sci* 96: 117-131. doi: 10.1016/B978-0-12-381280-3.00005-1
 19. Merchant JL, Ding L (2017) Hedgehog Signaling Links Chronic Inflammation to Gastric Cancer Precursor Lesions. *Cell Mol Gastroenterol Hepatol* 3 (2): 201-210. doi: 10.1016/j.jcmgh.2017.01.004
 20. Ge M, Zhang L, Cao L, Xie C, Li X, Li Y, Meng Y, Chen Y, Wang X, Chen J, Zhang Q, Shao J, Zhong C (2019) Sulforaphane inhibits gastric cancer stem cells via suppressing sonic hedgehog pathway. *Int J Food Sci Nutr* 70 (5): 570-578. doi: 10.1080/09637486.2018.1545012
 21. Peng Y, Zhang X, Lin H, Deng S, Qin Y, He J, Hu F, Zhu X, Feng X, Wang J, Wei Y, Fan X, Lin H, Ashktorab H, Smoot D, Lv Y, Li S, Meltzer SJ, Jin Z (2021) Dual activation of Hedgehog and Wnt/beta-catenin signaling pathway caused by downregulation of SUFU targeted by miRNA-150 in human gastric cancer. *Aging (Albany NY)* 13 (7): 10749-10769. doi: 10.18632/aging.202895
 22. Huang R, Yang Z, Liu Q, Liu B, Ding X, Wang Z (2022) CircRNA DDX21 acts as a prognostic factor and sponge of miR-1264/QKI axis to weaken the progression of triple-negative breast cancer. *Clinical and translational medicine* 12 (5): e768. doi: 10.1002/ctm2.768
 23. Chen D, Chou F-J, Chen Y, Tian H, Wang Y, You B, Niu Y, Huang C-P, Yeh S, Xing N, Chang C (2020) Targeting the radiation-induced TR4 nuclear receptor-mediated QKI/circZEB1/miR-141-3p/ZEB1 signaling increases prostate cancer radiosensitivity. *Cancer Letters* 495: 100-111. doi: https://doi.org/10.1016/j.canlet.2020.07.040
 24. Zong FY, Fu X, Wei WJ, Luo YG, Heiner M, Cao LJ, Fang Z, Fang R, Lu D, Ji H, Hui J (2014) The RNA-binding protein QKI suppresses cancer-associated aberrant splicing. *PLoS genetics* 10 (4): e1004289. doi: 10.1371/journal.pgen.1004289
 25. Bian Y, Wang L, Lu H, Yang G, Zhang Z, Fu H, Lu X, Wei M, Sun J, Zhao Q, Dong G, Lu Z (2012) Downregulation of tumor suppressor QKI in gastric cancer and its implication in cancer prognosis. *Biochemical and Biophysical Research Communications* 422 (1): 187-193. doi: https://doi.org/10.1016/j.bbrc.2012.04.138
 26. Han B, Wang R, Chen Y, Meng X, Wu P, Li Z, Duan C, Li Q, Li Y, Zhao S, Jiang C, Cai J (2019) QKI deficiency maintains glioma stem cell stemness by activating the SHH/GLI1 signaling pathway. *Cellular oncology (Dordrecht)* 42 (6): 801-813. doi: 10.1007/s13402-019-00463-x
 27. Zeng X, Xiao J, Bai X, Liu Y, Zhang M, Liu J, Lin Z, Zhang Z (2022) Research progress on the circRNA/lncRNA-miRNA-mRNA axis in gastric cancer. *Pathology, research and practice* 238: 154030. doi: 10.1016/j.prp.2022.154030
 28. Zhu G, Chang X, Kang Y, Zhao X, Tang X, Ma C, Fu S (2021) CircRNA: A novel potential strategy to treat thyroid cancer (Review). *International journal of molecular medicine* 48 (5). doi: 10.3892/ijmm.2021.5034
 29. Huang Z, Ma W, Xiao J, Dai X, Ling W (2021) CircRNA_0092516 regulates chondrocyte proliferation and apoptosis in osteoarthritis through the miR-337-3p/PTEN axis. *Journal of biochemistry* 169 (4): 467-475. doi: 10.1093/jb/mvaa119
 30. Dong Z, Liu Z, Liang M, Pan J, Lin M, Lin H, Luo Y, Zhou X, Yao W (2021) Identification of circRNA-miRNA-mRNA networks contributes to explore underlying pathogenesis and therapy strategy of gastric cancer. *Journal of translational medicine* 19 (1): 226. doi: 10.1186/s12967-021-02903-5
 31. Huang G, Liang M, Liu H, Huang J, Li P, Wang C, Zhang Y, Lin Y, Jiang X (2020) CircRNA hsa_circRNA_104348 promotes hepatocellular carcinoma progression through modulating miR-187-3p/RTKN2 axis and activating Wnt/ β -catenin pathway. *Cell death & disease* 11 (12): 1065. doi: 10.1038/s41419-020-03276-1